

Communication

## Polydimethylsiloxane (PDMS) Coating onto Magnetic Nanoparticles Induced by Attractive Electrostatic Interaction

Carina Sötebier, Aude Michel and Jérôme Fresnais \*

Physicochimie des Electrolytes, Colloïdes et Sciences Analytiques, UMR 7195, 4 place Jussieu - cc51 75252 Paris cedex 05, France

\* Author to whom correspondence should be addressed; E-Mail: jerome.fresnais@upmc.fr;  
Tel.: +33-01-4427-4309; Fax: +33-01-4427-3228.

Received: 16 March 2012; in revised form: 7 May 2012 / Accepted: 21 May 2012 /

Published: 29 May 2012

---

**Abstract:** In this article, we present an efficient synthesis pathway of polydimethylsiloxane (PDMS) coated magnetic nanoparticles from hydrophilic polyacrylate coated ferrofluids (NPPAA). A block copolymer based on polydimethylsiloxane is selected for its propensity to interact with the carboxylate functions on the NPPAA. The interaction is due to negative charges on NPPAA and positive ones on the amphiphilic copolymer. The synthesis is achieved by interfacial interaction, simplifying the purification of the PDMS-coated nanoparticles (NPPDMS) from subproducts such as ions and water. NPPDMS are well dispersed in hydrophobic solvents (toluene, diethyl ether) and can then be embedded into a curable PDMS polymer.

**Keywords:** magnetic nanoparticle; PDMS; amphiphilic copolymer; electrostatic complexation; polydimethylsiloxane composite; aminopropylsiloxane

---

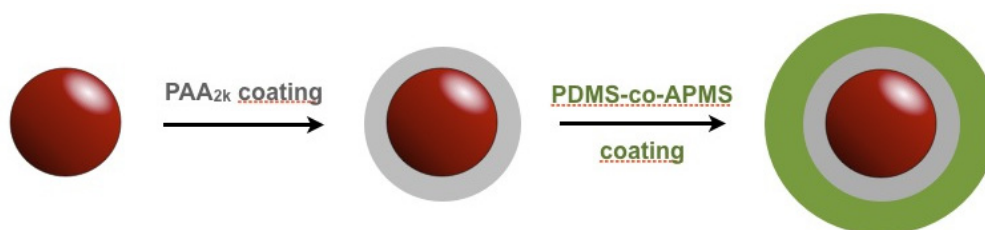
### 1. Introduction

Magnetic nanoparticles are widely used as multifunctional materials for magnetic separation, catalysis, MRI contrast agents and vectorization. They can be embedded in polymers such as PDMS to form functional elastomers, which combine the properties of the matrix and the nanoparticles [1,2]. Incorporating well-dispersed nanoparticles into a polymeric matrix is, however, not an easy task [3–6]. When nanoparticles are mixed with polymer melts or polymer solutions, depletion of the free chains in close vicinity of one another [7] can occur. This is mainly the case when the nanoparticle surface is not

efficiently stabilized. As a result, nanoparticles must be compatibilized with the selected polymer matrix, for instance by grafting a polymer layer onto the surface [8–10]. The length of the grafted polymer also has an important role [4,7,11,12]. In the case of a curable polymer matrix such as PDMS, obtaining very fine dispersions are rendered more difficult due to the polymer's low surface energy. Different strategies were used to overcome this issue [2,9,13–15]. The use of oleic acid is a good pathway to disperse nanoparticles into this hydrophobic polymer [16–18]. However, a long mixing time with different solvents is needed. Other results showed that grafting from or grafting onto methods can be done with success to overcome aggregation [19–21]. In this case, small quantities of functionalized nanoparticles are obtained, mainly because the grafting method starts from diluted dispersions.

Here we propose a versatile and easy method to compatibilize nanoparticles with a PDMS matrix. First, polyacrylic acid polymer (2,100 g/mol, noted PAA2k) is selected to stabilize iron oxide nanoparticles in water [22,23] at pH from 4 to 11. We already demonstrated that this coating provides both stability and post functionalization to prepare controlled aggregates, either spherical [24] or elongated [25,26]. In a second step, aminopropylmethylsiloxane-*co*-dimethylsiloxane block copolymer (PDMS-*co*-APMS) is used to add a hydrophobic coating to the NPPAA (Figure 1). These nanoparticles (called NPPDMS, for nanoparticles coated first with PAA2K, then with PDMS-*co*-APMS) are easily dispersed into a PDMS matrix without adding solvent. The corona thickness is directly governed by the molecular weight of the PDMS copolymer. Contrary to grafting onto or grafting from methods, this synthesis pathway gives rise to large numbers of functional nanoparticles in a few hours.

**Figure 1.** Scheme of the PAA2k and PDMS-*co*-APMS coating on iron oxide nanoparticles.



## 2. Experimental Section

### 2.1. Nanoparticle Synthesis and PAA Coating

The synthesis of magnetic nanoparticles is based on the condensation of iron II and iron III salts in ammonia, yielding to the formation of magnetite nanoparticles. Magnetite is oxidized into maghemite by reacting with iron III nitrate at 80 °C for one hour. Typically, the maghemite ( $\gamma\text{-Fe}_2\text{O}_3$ ) nanoparticle size distribution, with size comprised between 4 and 15 nm [27,28], is described by a lognormal distribution, with a polydispersity of 0.35. At pH 2, the maghemite nanoparticles are stabilized by electrostatic interactions arising from the native cationic charges at the surface of the particles. From this synthesis, size sorting is achieved to obtain different parts with smaller size distributions [28]. Particle sizes and size distributions were characterized by vibrating sample magnetometry, electron microscopy, and dynamic light scattering. The nanoparticles put under scrutiny presented a median

diameter  $D_{NP} = 7.8$  nm and a polydispersity  $\sigma = 0.19$ , determined by TEM. In order to improve their colloidal stability at neutral pH in water and to control their association with the PDMS-based copolymer, magnetic nanoparticles are coated with oppositely charged polyelectrolyte, namely polyacrylic acid with a molecular weight of  $2,100 \text{ g}\cdot\text{mol}^{-1}$  (Sigma Aldrich).

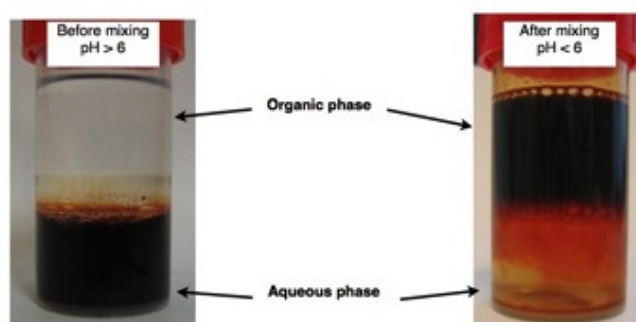
This synthesis followed the precipitation redispersion process described previously [22]. The precipitation of the cationic  $\gamma\text{-Fe}_2\text{O}_3$  dispersion by PAA2K was performed by mixing the acidic solution of PAA2K (1 wt.%) and the acidic nanoparticle dispersion (1 wt.%) at a 2:1 weight ratio (excess of polymer). After elimination of the clear supernatant, the pH was increased by addition of ammonium hydroxide. As a consequence, the precipitate redispersed spontaneously, yielding to PAA2k-coated nanoparticles (NPPAA2K).

Those nanoparticles were dialyzed against water in membrane of porosity 10kD (Slyde-A-Lyzer, Thermo scientific) in order to remove the unlinked PAA2k polymer chains from the nanoparticle dispersion. This point is crucial in order to prevent reaction between the PDMS-based copolymer and the free PAA chains.

## 2.2. Nanoparticle Coating with PDMS-co-APMS

The second step of the nanoparticle coating is undertaken by phase extraction of the nanoparticles from the aqueous phase to the organic one (typically diethyl ether containing the PDMS-co-APMS copolymer). Different block copolymers were selected in order to functionalize the PAA coated nanoparticles. Aminopropylmethylsiloxane-co-dimethylsiloxane copolymer with 2–3%, 4–5%, and 6–7% of amino groups were taken from Gelest. Their viscosities are 80–120 cSt, 100–300 cSt, and 80–200 cSt, respectively. The PDMS-co-APMS block copolymers are dissolved in ethyl ether at a weight fraction of 1%. This solvent is chosen for its density lower than water, so that nanoparticles can be recovered in the upper phase when the reaction is achieved. NPPAA dispersion (1 wt.%) is put in a vial (bottom phase). The PDMS-co-APMS solution is added and the two phases are mixed gently by magnetic stirring. Then, the pH of the aqueous phase is decreased to 5.5 by adding nitric acid (0.1 mol/L). Nanoparticles are spontaneously extracted to the upper phase (Figure 2). The diethyl ether dispersion is then separated, dried onto  $\text{MgSO}_4$  to remove water, and filtered. Solvent is removed using a rotavapor. A viscous magnetic paste is obtained.

**Figure 2.** Vials containing the two phases before (**left**) and after (**right**) pH decrease in the aqueous phase.



### 3. Results and Discussion

#### 3.1. The Coatings of Nanoparticle and Their Characterization

PAA2K coating is the first to be taken into consideration. This coating was well described in previous articles, and gave a good stability to nanoparticles [22,23]. Its thickness was estimated by light scattering, comparing the hydrodynamic diameters from bare and coated nanoparticles (Table 1). Bare nanoparticles were measured at 11.6 nm, while PAA-coated nanoparticles measured 20.5 nm. The difference in size is due to the PAA2K layer that corresponds to 4.45 nm. This thickness is almost compatible with the length of the PAA2K chains with 22 monomers (for 2.1 kg/mol PAA2K polymer).

**Table 1.** Hydrodynamic diameters of bare, PAA and PAA/PDMS-*co*-APMS coated nanoparticles.

Bare nanoparticles			SC-PAA			SC-PAA-APMS		
Amine content	Diameter [nm]	PDI	Diameter [nm]	PDI	Thickness of coating [nm]	Diameter [nm]	PDI	Thickness of coating [nm]
2–3%	11.6	0.16	20.5	0.17	4.5	41.6	0.14	10.6
4–5%	11.6	0.16	20.5	0.17	4.5	84.2	0.28	32
6–7%	11.6	0.16	20.5	0.17	4.5	66.9	0.27	23.2

NPPAA were then coated with the PDMS-*co*-APMS copolymer. The method described here, consisting of extracting nanoparticles from water to an organic solvent, was successfully achieved by other teams using surfactants [29,30]. Meriguet *et al.* used sodium dodecyl sulfate (SDS) molecules, which interacted with nanoparticles by electrostatic interactions. However, one main drawback is that SDS is soluble in both water and organic solvents. In this case, it is very difficult to establish whether all SDS molecules are involved in the nanoparticle coating or not. In our case, the PDMS-*co*-APMS copolymer selected is only soluble in organic solvents, so that we can easily manage the quantity of the copolymer added to the diethyl ether solution. The whole copolymer is attached to the nanoparticles when the aqueous phase conserves only a little orange color, indicating the presence of a small amount of nanoparticles.

Meriguet *et al.* [29] also shed light on the fact that the coating of nanoparticles is complete when no emulsion is left in the vial after mixing. Because emulsions are always difficult to destabilize and wash, we operated with gentle mixing and adjusted the amount of PDMS-*co*-APMS to coat the whole nanoparticle surface. As a consequence, either small or no polymer excess is obtained during this synthesis. This reaction is conducted in a few minutes and the purification process is achieved in less than one hour.

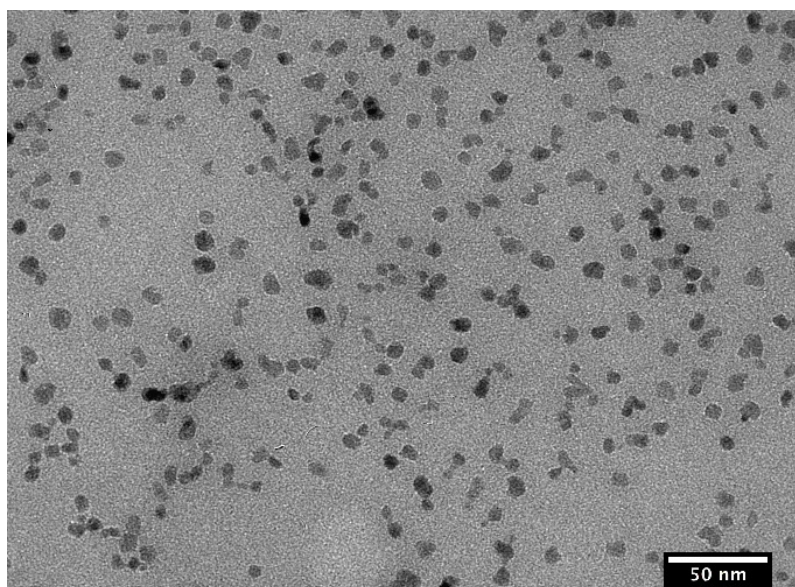
To understand the efficiency of this coating, one can consider the interaction that occurred between carboxylate functions of the PAA2K chains and the amine functions of the PDMS-*co*-APMS copolymer. These amine functions can react with the negative carboxylate functions by electrostatic interaction only if they are positively charged. This is facilitated by decreasing the pH of the water phase lower than their pKa. Typical pKa of amine are in the range of 9–11. As an example, this pKa is measured above 9 for amine containing polymers, but decreased to 7.2 when the amines are close to the surface [31]. For the copolymer scrutinized in this study, the pKa should be at a comparable value. Reactivity of such an amine is maximum for 2 pH units above its pKa. The reaction can be achieved

only if the pH is lower than 6–7. This was experimentally observed in our case. The interaction occurred at a pH lower than 6.

However, the pH must not be too low to ensure nanoparticle stability. Indeed, the PAA2k-coated nanoparticles are stable with pH higher than 4.5 [22]. For this reason, the pH was adjusted to 5.5 during the experiment by adding small amounts of 0.1 M nitric acid solution. At this value, nanoparticles change spontaneously from the aqueous phase to the organic one (Figure 2).

For this study, three block copolymers were used. They were selected to get a short or a long PDMS corona on the nanoparticles. This is of uttermost importance, in order to manage the attractive and repulsive interaction between nanoparticles. For the magnetic nanoparticles selected in this study, no strong magnetic attraction is expected. But in the case of large or ferromagnetic nanoparticles, the steric repulsion must be strong enough to prevent the nanoparticles from magnetic aggregation. The copolymers differed with their aminopropyl proportion, which are 2–3%, 4–5%, and 6–7%. According to the light-scattering experiments achieved in good solvent for PDMS (diethyl ether—Table 1), the PDMS-*co*-APMS thicknesses are 10.6, 32, and 23.2 nm, respectively. The kinematic viscosities of the three copolymer are 80–120 cSt for 2–3% and 6–7% copolymers, and 150–300 cSt for 4–5% copolymer. For siloxane polymers, their molecular weight is directly proportional to their viscosity. We can then emphasize that the 4–5% copolymer is longer than the other two, explaining the thicker coating on the 4–5% NPPDMS. The good dispersion is confirmed with TEM images showing no evident aggregation for nanoparticles coated with 4–5% PDMS-*co*-APMS copolymer (Figure 3).

**Figure 3.** TEM images of (4–5%) PDMS-*co*-APMS-coated nanoparticle dispersion.



This easy and reproducible synthesis technique provided batches of nanoparticles that are stable and well dispersed with the three copolymers selected. The strong advantage is that no residual solvent remained after solvent evaporation. As a consequence, low dilution can be obtained when nanoparticles are mixed in a PDMS matrix. This is what will be explored in the following part of this article.

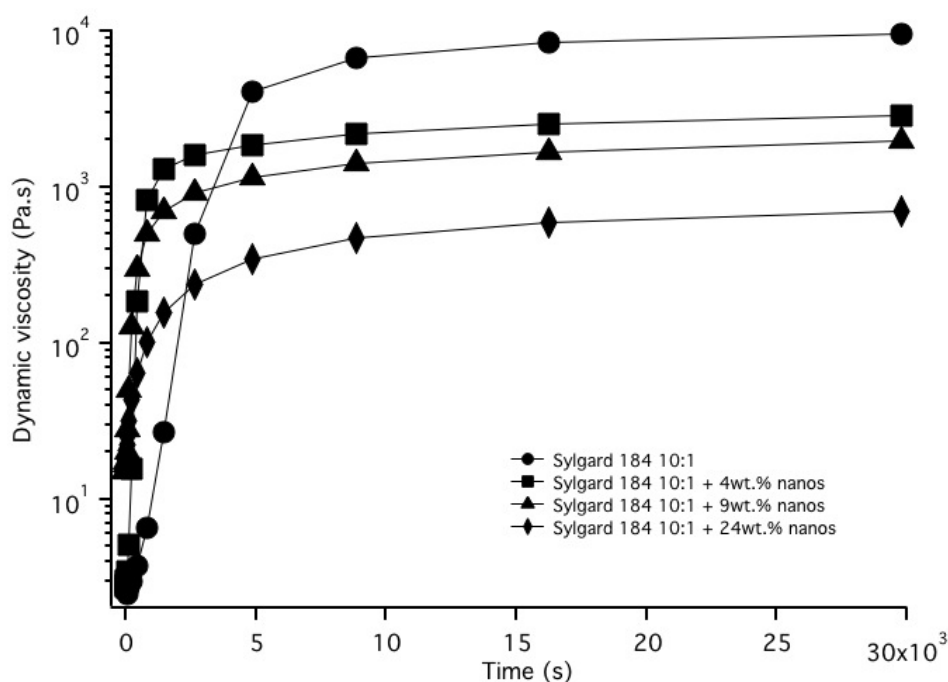
### 3.2. Nanoparticle Incorporation into PDMS Matrix

PDMS is a cross-linkable polymer widely used in microfluidics. Magnetic PDMS is intended to be used in pumping or actuating systems in micro-systems [2,6,14,15,32]. The main PDMS used in microfluidics is the Sylgard 184, which allows good elasticity and mechanical stability. This polymer can be crosslinked by the mixture of two components in a ratio 10:1. Studies have shown that polymer chains grafted onto nanoparticles should be longer than the matrix chains in order to have a good dispersion with a swollen corona [20,33]. In the case of Sylgard 184, a mixture of almost six components complicates the interpretation in terms of particle distribution in the matrix. The crosslinking reaction is achieved with platinum catalyst that allows the reaction between Si-H bound and carbon-carbon double bounds.

The PDMS-*co*-APMS copolymer used in this study contained no such chemical function. As a consequence, nanoparticles will not interact with the chemical backbone of the PDMS matrix. For this reason, two cases can be considered. First, NPPDMS are smaller than the reticulated matrix mesh size, and the reticulation should not be changed, leading to no change in elastic modulus of the loaded Sylgard 184. Secondly, NPPDMS are larger than the matrix mesh size. In this case, the reticulation process should be impeached by the nanoparticles. The more particles, the smaller the elastic modulus should be.

We achieved experiments with Sylgard 184 and its crosslinker in the ratio 10:1, adding 4%, 9%, and 24% by weight of magnetic nanoparticles coated with 4–5% PDMS-*co*-APMS. Dynamic viscosity was measured *versus* time by rheometry at 70 °C on a plane-plane rheometer (rheoptical rheometer, Thermo-Haake) by oscillations at 10 Hz with a strain fixed at 10 Pa during reticulation (Figure 4).

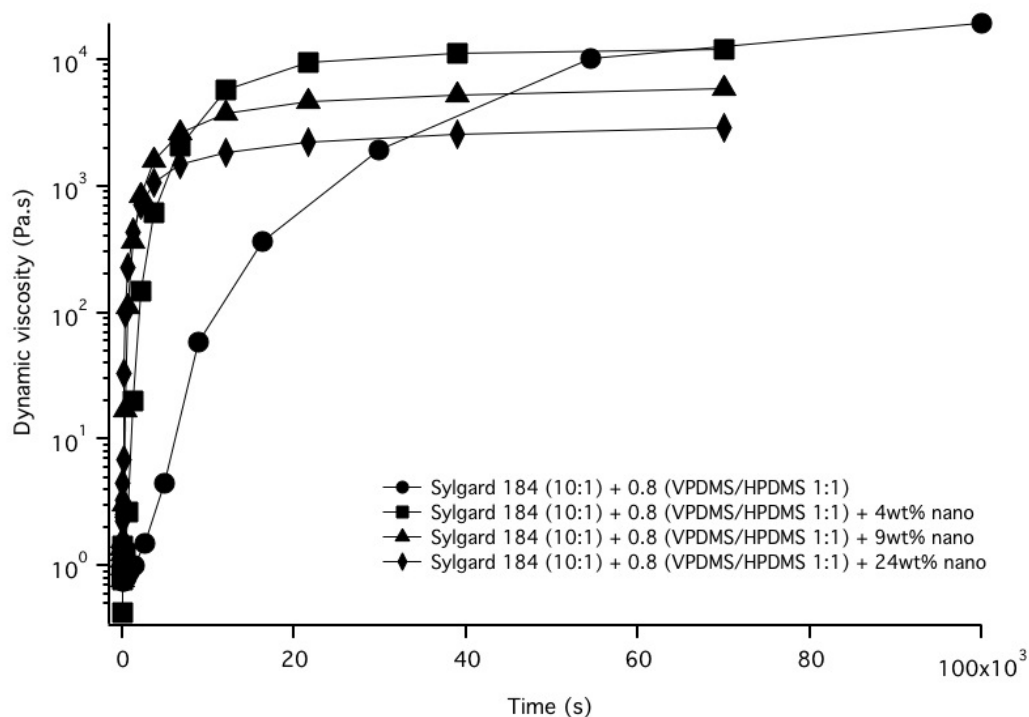
**Figure 4.** Dynamic viscosity *versus* time for Sylgard 184 reticulation without and with 4 wt %, 9 wt %, and 24 wt% of magnetic nanoparticles coated with 4–5% PDMS-*co*-APMS.



The viscosity plateau is expected when complete reticulation is reached. This appeared for pristine Sylgard in 15,000 s with a plateau at  $10^4$  Pa·s. For the PDMS mixtures containing magnetic nanoparticles, two observations are noticed. Firstly, the reticulation appeared at shorter times. This could be due to a catalytic effect of the nanoparticles in the matrix. Secondly, the higher the proportion of nanoparticles, the lower the viscosity at the plateau. As an example, the plateau dynamic viscosity decreased from  $10^4$  Pa·s for unloaded matrix to 500 Pa·s for the PDMS matrix loaded with 24 wt.% of nanoparticles. NPPDMS clearly induced a decrease of the mechanical properties of the reticulated Sylgard 184 matrix.

To overcome this diminution of mechanical properties, we made different formulations with copolymers that contain Si-H and carbon-carbon double bounds. They acted as a crosslinker in the matrix. Two copolymers were selected, which are poly(hydromethylsiloxane-*co*-dimethylsiloxane) with 7–8 % (HPDMS) of Si-H functions copolymer and poly(vinylmethylsiloxane-*co*-dimethylsiloxane) copolymer with 7–8 % of vinyl functions (VPDMS). An optimization of the formulation, which is not detailed here, gave the best results in terms of elasticity and non-stickiness for one part by mass of Sylgard 184 10:1 mixed with 0.8 part by mass of the mixture VPDMS/HPDMS in the ratio 1:1. Same experiments as the one presented in Figure 4 were performed with this formulation (Figure 5).

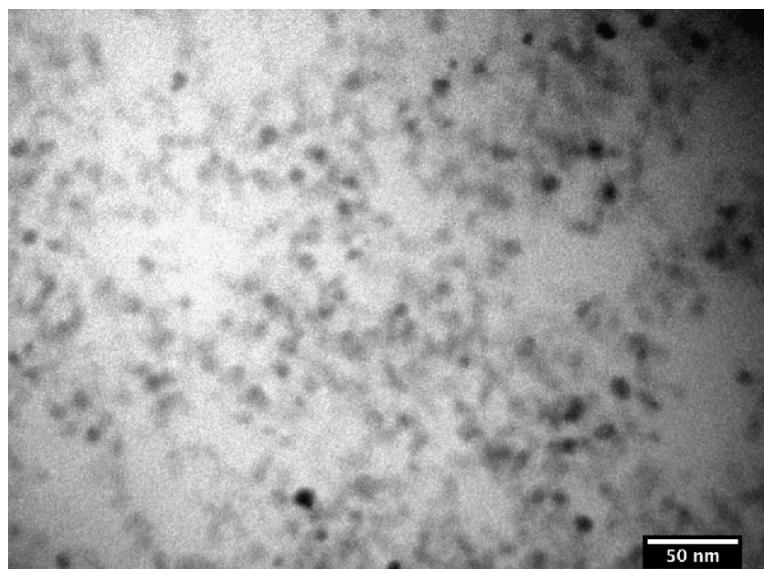
**Figure 5.** Dynamic viscosity *versus* time for Sylgard 184 with (HPDMS:VPDMS) (mixture ratio 1:0.8) reticulation without and with 4 wt%, 9 wt%, and 24 wt% of magnetic nanoparticles coated with 4–5% PDMS-*co*-APMS



The reticulation of the Sylgard and the VPDMS/HPDMS mixture is very slow, even compared to the pure Sylgard matrix reticulation. However, the same viscosity plateau is reached for those two matrixes. As shown for the Sylgard matrix, nanoparticles increased the reticulation rate, compared to the matrix. For a comparable quantity of nanoparticles, the plateau viscosities are strongly increased

when nanoparticles are mixed with the modified matrix. As an example, Sylgard with 24 wt.% of nanoparticles is 50 times less viscous than the modified matrix. This is explained by a higher reticulation due to the addition of a crosslinker copolymer in the mixture. Cryo-microtomy and TEM experiments (on a FEI Tecnai F20 ST microscope) on this magnetic PDMS matrix showed that the nanoparticles are well dispersed (Figure 6).

**Figure 6.** TEM images of (4–5%) NPPMDS in modified Sylgard reticulated matrix (scale bar: 100 nm).



We demonstrated that NPPDMS put under scrutiny were larger than the mesh size of the Sylgard 184 network. By modifying the formulation of this Sylgard 184 by adding two co-reticulated copolymers, we demonstrated that magnetic PDMS matrix could be prepared with good mechanical properties with a large quantity of magnetic nanoparticles.

#### 4. Conclusions

To conclude, we demonstrated that PAA2k-coated nanoparticles can be coated with a PDMS-based copolymer, yielding to hydrophobized nanoparticles that can be dispersed in a Sylgard matrix. The sizes of both PAA2k and PDMS corona were measured by dynamic light scattering. Depending on the proportion of amino groups in the chains, different PDMS corona thicknesses can be determined, from 10 to 32 nm. Those nanoparticles can be mixed with Sylgard 184 matrix, but the presence of the nanoparticles gave rise to a decrease in the viscosity of the reticulated matrix, or a decrease in its elastic and viscous modulus. To overcome this effect, we propose a formulation that contains two copolymers that increase the modulus of the nanoparticle loaded matrix by a factor of 50 for a 24 wt% nanoparticle content.

Those magnetically loaded matrixes could be used in microfluidics for the entrapment of magnetic particles circulating in a microchannel, as actuators or as a pumping system.

## Acknowledgments

We would like to thank Véronique Peyre for fruitful discussions. Eric Leroy is acknowledged for cryo-microtomy and TEM images on the magnetic PDMS matrix.

## References

1. Denver, H.; Heiman, T.; Martin, E.; Gupta, A.; Borca-Tasciuc, D.A. Fabrication of polydimethylsiloxane composites with nickel nanoparticle and nanowire fillers and study of their mechanical and magnetic properties. *J. Appl. Phys.* **2009**, *106*, 64909:1–64909:5.
2. Antonel, P.S.; Jorge, G.; Perez, O.E.; Butera, A.; Leyva, A.G.; Negri, R.M. Magnetic and elastic properties of  $\text{CoFe}_2\text{O}_4$  polydimethylsiloxane magnetically oriented elastomer nanocomposites. *Macromol. Rapid Commun.* **2011**, *110*, 43920:1–43920:8.
3. Mefford, O.T.; Carroll, M.R.J.; Vadala, M.L.; Goff, J.D.; Mejia-Ariza, R.; Saunders, M.; Woodward, R.C.; St Pierre, T.G.; Davis, R.M.; Riffle, J.S. Size analysis of PDMS-magnetite nanoparticle complexes: Experiment and theory. *Chem. Mater.* **2008**, *20*, 2184–2191.
4. Mefford, O.T.; Vadala, M.L.; Goff, J.D.; Carroll, M.R.J.; Mejia-Ariza, R.; Caba, B.L.; St Pierre, T.G.; Woodward, R.C.; Davis, R.M.; Riffle, J.S. Stability of polydimethylsiloxane-magnetite nanoparticle dispersions against flocculation: Interparticle interactions of polydisperse materials. *Langmuir* **2008**, *24*, 5060–5069.
5. Miles, W.C.; Goff, J.D.; Huffstetler, P.P.; Mefford, O.T.; Riffle, J.S.; Davis, R.M. The design of well-defined PDMS-Magnetite complexes. *Polymer* **2009**, *51*, 482–491.
6. Wilson, K.S.; Goff, J.D.; Riffle, J.S.; Harris, L.A.; St Pierre, T.G. Polydimethylsiloxane-magnetite nanoparticle complexes and dispersions in polysiloxane carrier fluids. *Polym. Advan. Technol.* **2005**, *16*, 200–211.
7. Dutta, N.; Green, D. Nanoparticle stability in semidilute and concentrated polymer solutions. *Langmuir* **2008**, *24*, 5260–5269.
8. Aqil, A.; Vasseur, S.; Duguet, E.; Passirani, C.; Benoit, J.P.; Roch, A.; Muller, R.; Jerome, R.; Jerome, C. PEO coated magnetic nanoparticles for biomedical application. *Eur. Polym. J.* **2008**, *44*, 3191–3199.
9. Borrell, M.; Leal, L.G. Interfacial activity of polymer-coated gold nanoparticles. *Langmuir* **2007**, *23*, 12497–12502.
10. Vadala, M.L.; Rutnakornpituk, M.; Zalich, M.A.; St Pierre, T.G.; Riffle, J.S. Block copolysiloxanes and their complexation with cobalt nanoparticles. *Polymer* **2004**, *45*, 7449–7461.
11. Ditsch, A.; Laibinis, P.E.; Wang, D.I.C.; Hatton, T.A. Controlled clustering and enhanced stability of polymer-coated magnetic nanoparticles. *Langmuir* **2005**, *21*, 6006–6018.
12. Galicia, J.A.; Sandre, O.; Cousin, F.; Guemghar, D.; Menager, C.; Cabuil, V. Designing magnetic composite materials using aqueous magnetic fluids. *J. Phys.-Condens. Matter.* **2003**, *15*, 1379–S1402.
13. Denver, H.; Heiman, T.; Martin, E.; Gupta, A.; Borca-Tasciuc, D.A. Mechanical Characterization of Nickel Nanoparticles Elastomer Composites. In *Nsti Nanotech 2008*; Anaheim, Canada, 2008; pp. 301–303.

14. Evans, B.A.; Shields, A.R.; Carroll, R.L.; Washburn, S.; Falvo, M.R.; Superfine, R. Magnetically actuated nanorod arrays as biomimetic cilia. *Nano Lett.* **2007**, *7*, 1428–1434.
15. Goyal, A.; Kumar, A.; Patra, P.K.; Mahendra, S.; Tabatabaei, S.; Alvarez, P.J.J.; John, G.; Ajayan, P.M. *In Situ* synthesis of metal nanoparticle embedded free standing multifunctional PDMS films. *Macromol. Rapid Commun.* **2009**, *30*, 1116–1122.
16. Lattuada, M.; Hatton, T.A. Functionalization of monodisperse magnetic nanoparticles. *Langmuir* **2007**, *23*, 2158–2168.
17. Yang, T.I.; Brown, R.N.C.; Ckempel, L.; Kofinas, P. Controlled synthesis of core-shell iron-silica nanoparticles and their magneto-dielectric properties in polymer composites. *Nanotechnology* **2011**, *22*, 105601:1–105601:8.
18. Zhang, L.; He, R.; Gu, H.C. Oleic acid coating on the monodisperse magnetite nanoparticles. *Appl. Surf. Sci.* **2006**, *253*, 2611–2617.
19. Bell, N.S.; Frischknecht, A.L.; Piech, M. Grafted low molecular weight polymers as steric stabilizers of commercial titania nanoparticles in polydimethylsiloxane fluids. *J. Disper. Sci. Tech.* **2010**, *32*, 128–140.
20. Prucker, O.; Ruhe, J. Synthesis of poly(styrene) monolayers attached to high surface area silica gels through self-assembled monolayers of azo initiators. *Macromolecules* **1998**, *31*, 592–601.
21. Valentine, M.T.; Perlman, Z.E.; Gardel, M.L.; Shin, J.H.; Matsudaira, P.; Mitchison, T.J.; Weitz, D.A. Colloid surface chemistry critically affects multiple particle tracking measurements of biomaterials. *Biophys. J.* **2004**, *86*, 4004–4014.
22. Sehgal, A.; Lalatonne, Y.; Berret, J.-F.; Morvan, M. Precipitation-redispersion of cerium oxide nanoparticles with poly(acrylic acid): Toward stable dispersions. *Langmuir* **2005**, *21*, 9359–9364.
23. Chanteau, B.; Fresnais, J.; Berret, J.F. Electrosteric enhanced stability of functional sub-10 nm cerium and iron oxide particles in cell culture medium. *Langmuir* **2009**, *25*, 9064–9070.
24. Fresnais, J.; Lavelle, C.; Berret, J.F. Nanoparticle aggregation controlled by desalting kinetics. *J. Phys. Chem.* **2009**, *113*, 16371–16379.
25. Fresnais, J.; Berret, J.F.; Frka-Petesic, B.; Sandre, O.; Perzynski, R. Electrostatic co-assembly of iron oxide nanoparticles and polymers: Towards the generation of highly persistent superparamagnetic nanorods. *Advan. Mater.* **2008**, *20*, 3877–3881.
26. Frka-Petesic, B.; Fresnais, J.; Berret, J.F.; Dupuis, V.; Perzynski, R.; Sandre, O. Stabilization and controlled association of superparamagnetic nanoparticles using block copolymers. *J. Magn. Magn. Mater.* **2009**, *321*, 667–670.
27. Bee, A.; Massart, R.; Neveu, S. Synthesis of very fine maghemite particles. *J. Magn. Magn. Mat.* **1995**, *149*, 6–9.
28. Massart, R.; Dubois, E.; Cabuil, V.; Hasmonay, E. Preparation and properties of monodisperse magnetic fluids. *J. Magn. Magn. Mat.* **1995**, *149*, 1–5.
29. Mériguet, G.; Dubois, E.; Perzynski, R. Liquid-liquid phase-transfer of magnetic nanoparticles in organic solvents. *J. Coll. Int. Sci.* **2003**, *267*, 78–85.
30. Machunsky, S.; Grimm, P.; Schmid, H.J.; Peuker, U.A. Liquid-liquid phase transfer of magnetite nanoparticles. *Colloid. Surface. A.* **2009**, *348*, 186–190.

31. Abiman, P.; Wildgoose, G.G.; Crossley, A.; Jones, J.H.; Compton, R.G. Contrasting pKa of protonated bis(3-aminopropyl)-terminated polyethylene glycol “Jeffamine” and the associated thermodynamic parameters in solution and covalently attached to graphite surfaces. *Chem. Eur. J.* **2007**, *13*, 9663–9667.
32. Xiangli, F.J.; Chen, Y.W.; Jin, W.Q.; Xu, N.P. Polydimethylsiloxane (PDMS)/ceramic composite membrane with high flux for pervaporation of ethanol-water mixtures. *Ind. Eng. Chem. Res.* **2007**, *46*, 2224–2230.
33. Douadi-Masrouki, S.; Frka-Petesic, B.; Sandre, O.; Cousin, F.; Dupuis, V.; Perzynski, R.; Cabuil, V. Neutron reflectivity on polymer multilayers doped with magnetic nanoparticles. In *Magnetism and Magnetic Materials*; Perov, N., Ed.; Trans Tech Publications Ltd.: Stafa-Zurich, Switzerland, 2009; Volume 152–153, pp. 194–197.

© 2012 by the authors; licensee MDPI, Basel, Switzerland. This article is an open access article distributed under the terms and conditions of the Creative Commons Attribution license (<http://creativecommons.org/licenses/by/3.0/>).